

Coexistence of Topological Anderson Insulator and Multifractal Critical Phase in a Non-Hermitian Quasicrystal

Qi-Bo Zeng^{1*} and Rong Lü^{2,3}

¹*Department of Physics, Capital Normal University, Beijing 100048, China*

²*State Key Laboratory of Low-Dimensional Quantum Physics,*

Department of Physics, Tsinghua University, Beijing 100084, China and

³*Collaborative Innovation Center of Quantum Matter, Beijing 100084, China*

The interplay of topology, disorder, and non-Hermiticity gives rise to phenomena beyond the conventional classification of quantum phases. We propose a one-dimensional non-Hermitian Su–Schrieffer–Heeger model with quasiperiodically modulated nonreciprocal intracell hopping. We show that quasiperiodic modulation can substantially enhance topological robustness and, remarkably, induce a non-Hermitian topological Anderson insulator (TAI) phase. Beyond the topological transition, increasing nonreciprocity drives a cascade of localization transitions in which all bulk eigenstates evolve from extended to multifractal critical and ultimately to localized states. Strikingly, the extended-to-critical transition coincides exactly with a real–complex spectral transition. We establish complete phase diagrams and derive exact analytical boundaries for both topological and localization transitions, uncovering an unanticipated coexistence of TAI and multifractal critical phases. Finally, we propose a feasible implementation in topoelectrical circuits. Our results reveal a new paradigm for the cooperative effects of topology, quasiperiodicity, and non-Hermiticity.

Introduction—The discovery of topological phases has fundamentally reshaped our understanding of quantum matter, revealing boundary states protected by global topological invariants [1–3]. While this framework was originally formulated for Hermitian systems, growing interest in open and dissipative platforms has propelled the development of non-Hermitian topology [4–7]. Non-Hermitian Hamiltonians naturally emerge in systems with gain and loss [8, 9], finite quasiparticle lifetimes [10], complex refractive indices in photonics [11, 12], and engineered Laplacians in electrical circuits [13–15]. In contrast to Hermitian counterparts, such systems host intrinsically non-Hermitian topological structures, including exceptional points [16] and complex-energy braiding [17–19]. Remarkably, they also support phases without Hermitian analogs [6, 7]. A defining feature of nonreciprocal systems is the breakdown of conventional bulk–boundary correspondence due to the non-Hermitian skin effect (NHSE), where an extensive number of eigenstates accumulate at the boundaries [20, 21]. The NHSE itself has a topological origin, intimately connected to point-gap topology under periodic boundary conditions [22, 23].

Disorder, ubiquitous in realistic systems, generally destabilizes topological phases through Anderson localization [24]. Yet disorder can also play a constructive role: sufficiently strong randomness may induce topological transitions from trivial phases, leading to the topological Anderson insulator (TAI) [25–41]. The interplay between disorder and non-Hermiticity further enriches localization physics, producing unconventional spectral and transport behavior [42–47]. Extending the TAI paradigm to non-Hermitian systems has revealed a diverse landscape of disorder-driven topological transitions [48–52]. In parallel, quasiperiodic systems such as

the André–Aubry–Harper model [53, 54] provide a deterministic route to localization transitions. With suitable quasiperiodic modulations or long-range hopping, quasicrystals can host mobility edges separating extended and localized states [55–59]. The associated critical states may proliferate into an intermediate multifractal phase, distinguished from both extended and localized regimes by its spectral statistics and wave-function scaling properties [60–67]. Such critical phases are central to nonergodic dynamics, anomalous transport, and many-body localization phenomena [68–71]. Topological states in quasiperiodic lattices have also been extensively investigated [72–80]. Despite these advances, a fundamental question remains unresolved: can a disorder-induced topological Anderson phase and a multifractal critical phase coexist within a unified non-Hermitian quasiperiodic framework? To date, these phenomena have largely been treated as distinct regimes, and the conditions enabling their simultaneous emergence remain unknown.

In this work, we resolve this question by introducing a one-dimensional non-Hermitian Su–Schrieffer–Heeger (SSH) model with quasiperiodically modulated nonreciprocal intracell hopping. We show that quasiperiodicity not only enhances the robustness of the topological phase but also drives a disorder-induced transition into a non-Hermitian TAI phase. More strikingly, increasing nonreciprocity induces a cascade of localization transitions, with all bulk eigenstates evolving from extended to multifractal critical and ultimately to localized regimes. The extended-to-critical transition coincides exactly with a real–complex spectral transition, establishing a direct correspondence between spectral feature and wave-function criticality. By deriving exact analytical phase boundaries, we construct the complete phase diagram and uncover a previously unexplored regime where

the TAI and multifractal critical phases coexist. Finally, we propose a feasible implementation in topoelectrical circuits, providing an experimentally accessible platform to probe the interplay of non-Hermiticity, topology, and quasiperiodic criticality.

Model Hamiltonian-We consider a one-dimensional SSH chain with quasiperiodically modulated nonreciprocal intracell hopping, described by

$$H = H_{SSH} + H_\lambda, \quad (1)$$

with

$$\begin{aligned} H_{SSH} &= \sum_j \left(vc_{j,A}^\dagger c_{j,B} + wc_{j,B}^\dagger c_{j+1,A} + h.c. \right), \\ H_\lambda &= \sum_j \left(\lambda \cos \theta_j c_{j,A}^\dagger c_{j,B} - \lambda \cos \theta_j c_{j,B}^\dagger c_{j,A} \right). \end{aligned} \quad (2)$$

Here, $c_{j,A(B)}$ creates a spinless fermion on sublattice $A(B)$ of the j th unit cell. The parameters v and w denote the intracell and intercell hopping amplitudes, respectively, while λ characterizes the strength of nonreciprocity. The modulation phase $\theta_j = 2\pi\alpha j + \phi$ introduces spatial inhomogeneity; for irrational α , the nonreciprocity is quasiperiodic. Throughout this work we take $\alpha = (\sqrt{5} - 1)/2$, $\phi = 0$, and set $w = 1$ as the energy unit. The lattice contains N unit cells ($L = 2N$ sites), and all parameters are real.

The Hamiltonian takes a tridiagonal non-Hermitian form under open boundary conditions. For $|\lambda| < |v|$, it can be mapped to a Hermitian matrix via a similarity transformation $h = D^{-1}HD$ with diagonal D [81] (see Supplemental Material (SM) [82]). Consequently, H is pseudo-Hermitian in the sense of Mostafazadeh [83], and its spectrum is entirely real in this regime. As illustrated in Fig. 1(a) and 1(b), the eigenenergies remain real for $|\lambda| < |v|$, while a real-complex spectral transition occurs at $|\lambda| = |v|$, beyond which the similarity transformation breaks down and complex eigenvalues emerge.

To characterize localization, we compute the inverse participation ratio (IPR) of the n th eigenstate, $\text{IPR}_n = \sum_{j,\alpha} (|\psi_{n,j}|^4 + |\psi_{n,j\alpha}|^4)$, with $\alpha = A, B$. In the thermodynamic limit, $\text{IPR}_n \rightarrow 0$ for extended states and remains finite for localized states. We further extract the fractal dimension, $\text{FD}_n = -\lim_{L \rightarrow \infty} [\ln \text{IPR}_n / \ln L]$, for which $\text{FD}_n = 1$ (0) corresponds to extended (localized) states, while $0 < \text{FD} < 1$ signals multifractal criticality. Note that there is no NHSE in our model due to that the nonreciprocity is quasiperiodic [84].

Transfer matrix and Lyapunov exponent-To analyze localization induced by quasiperiodic nonreciprocity, we formulate the transfer-matrix approach and compute the Lyapunov exponent. From the stationary Schrödinger equation $H|\psi\rangle = E|\psi\rangle$, with eigenstate $|\psi\rangle = \sum_j a_j |j, A\rangle + b_j |j, B\rangle$, yields

$$\begin{cases} Ea_j = (v + \lambda \cos \theta_j)b_j + wb_{j-1}, \\ Eb_j = (v - \lambda \cos \theta_j)a_j + wa_{j+1}. \end{cases} \quad (3)$$

Introducing the two-component vector

$$\Psi_j = \begin{pmatrix} a_j \\ b_{j-1} \end{pmatrix}, \quad (b_0 = 0), \quad (4)$$

the recursion relation can be written as

$$\Psi_{j+1} = T_E(\theta_j)\Psi_j, \quad (5)$$

with transfer matrix

$$T_E(\theta_j) = \frac{1}{w(v + \lambda \cos \theta_j)} \begin{pmatrix} E^2 - (v^2 - \lambda^2 \cos^2 \theta_j) & -Ew \\ Ew & -w^2 \end{pmatrix}. \quad (6)$$

The Lyapunov exponent is defined as

$$\gamma(E) = \lim_{N \rightarrow \infty} \frac{1}{N} \ln \left\| \prod_{j=1}^N T_E(\theta_j) \right\|, \quad (7)$$

where N is the number of unit cells and $\|\cdot\|$ denotes the matrix norm. The localization length is given by $\xi = \gamma^{-1}(E)$; thus $\gamma(E) > 0$ signals localization, while $\gamma(E) = 0$ corresponds to extended or critical states.

Topological Anderson insulator-For the clean SSH model ($\lambda = 0$), the system is topologically nontrivial when $|v| < |w|$. Introducing quasiperiodic nonreciprocity fundamentally alters this criterion. Remarkably, we find that a topological phase can emerge in the parameter regime that is trivial in the clean limit, thereby realizing a non-Hermitian topological Anderson insulator (TAI). Figure 1(c) shows the open-boundary spectrum $|E|$ as a function of λ when $v = 1.2 > w$, where the clean system is topologically trivial. As λ increases, zero-energy modes appear within a finite parameter window. Their spatial profiles [Fig. 1(f)] reveal two states exponentially localized at opposite ends of the chain, confirming the onset of a nontrivial topological phase induced by quasiperiodic nonreciprocity.

The topological transition can be determined analytically from the divergence of the localization length of the zero-energy modes. Setting $E = 0$ in Eq. (3), the Lyapunov exponent reduces to (see details in SM [82])

$$\gamma_0 = \lim_{N \rightarrow \infty} \frac{1}{N} \sum_{j=1}^N \ln \left| \frac{v - \lambda \cos \theta_j}{w} \right|. \quad (8)$$

Using phase averaging based on Weyl's equidistribution theorem and irrational rotations [85–87], we obtain

$$\gamma_0 = \begin{cases} \ln \frac{|\lambda|}{2|w|}, & |v| \leq |\lambda|; \\ \ln \frac{|v| + \sqrt{v^2 - \lambda^2}}{2|w|}, & |v| > |\lambda|. \end{cases} \quad (9)$$

The topological phase boundaries follow from $\gamma_0 = 0$,

$$|\lambda| = |2w|, \quad |v| + \sqrt{v^2 - \lambda^2} = 2|w|. \quad (10)$$

These expressions provide exact analytical criteria for the disorder-induced topological transition.

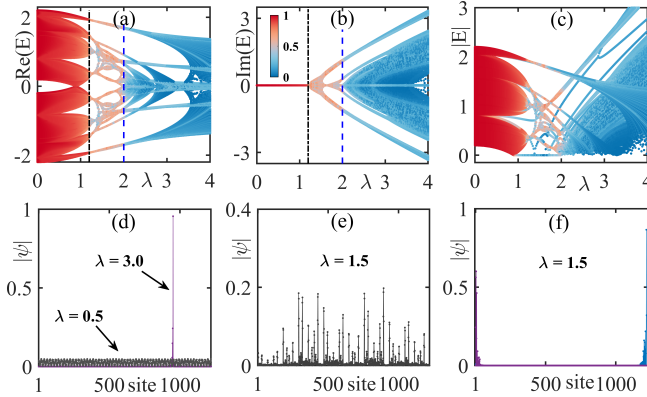


FIG. 1. (Color online) (a) Real and (b) imaginary parts of the eigenenergies under periodic boundary conditions as a function of the nonreciprocity strength λ . The black and blue dashed lines mark the critical values $\lambda = v$ and $\lambda = 2w$, separating the extended, multifractal critical, and localized regimes. The color scale indicates the fractal dimension FD of the corresponding eigenstates. (c) Energy spectrum $|E|$ under open boundary conditions. (d)–(e) Representative spatial profiles of eigenstates in the extended, critical, and localized phases, respectively. (f) Zero-energy edge modes in the topological Anderson insulating phase. Parameters: $v = 1.2$, $w = 1$, and system size $L = 2N = 1220$.

To further characterize the topological phase, we compute the real-space winding number under open boundary conditions [88]. The Hamiltonian preserves chiral symmetry, $SHS^{-1} = -H$, with $S = \sigma_z \otimes \mathcal{I}$. Let $|\psi_{nR}^\pm\rangle$ and $|\psi_{nL}^\pm\rangle$ denote the biorthonormal right and left eigenstates satisfying $H^\dagger|\psi_{nL}^\pm\rangle = \pm E_n^*|\psi_{nL}^\pm\rangle$ and $H^\dagger|\psi_{nR}^\pm\rangle = \pm E_n^*|\psi_{nR}^\pm\rangle$. Excluding edge modes, we define the open-boundary Q matrix as $Q = \sum_n (|\psi_{nR}^+\rangle\langle\psi_{nR}^+| - |\psi_{nL}^-\rangle\langle\psi_{nL}^-|)$, and the winding number

$$W = \frac{1}{2L'} \text{Tr}'(SQ[Q, X]), \quad (11)$$

where X is the coordinate operator and Tr' denotes the trace over a central region of length L' . We find $W = 1$ in the TAI phase and $W = 0$ in the trivial regime.

The resulting phase diagram in the $v - \lambda$ plane is shown in Fig. 2(a). The numerically obtained winding number agrees precisely with the analytical boundaries in Eq. (10), confirming the emergence of a disorder-induced topological phase.

Extended-critical-localized phase transitions. Quasiperiodic nonreciprocity also drives Anderson-type localization transitions. As shown in Figs. 1(a) and 1(b), the spectrum separates into three distinct regimes characterized by the fractal dimension FD of the eigenstates. For $v = 1.2$, all states are extended when $|\lambda| < 1.2$, become multifractal critical in the intermediate region $1.2 < |\lambda| < 2$, and are fully localized for $|\lambda| > 2$. Representative wave-function profiles are displayed in

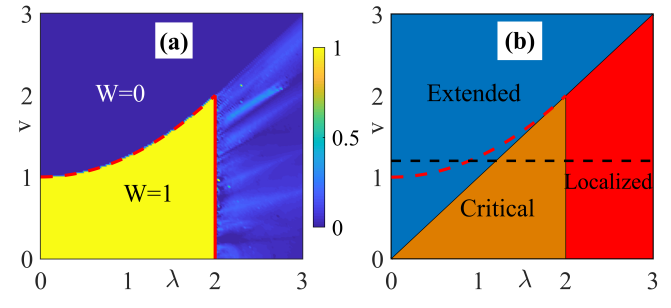


FIG. 2. (Color online) (a) Phase diagram in the $v - \lambda$ plane showing the topological Anderson insulating (TAI) and trivial phases. The color scale represents the real-space winding number W . Red dashed and solid lines denote the analytical phase boundaries given by Eq. (10). (b) Phase diagram of the extended, multifractal critical, and localized regimes determined from the Lyapunov exponent and fractal dimension. The black dashed line indicates the cut at $v = 1.2$.

Figs. 1(d) and 1(e), where the critical states exhibit clear multifractal spatial structures.

To quantify the transition, we compute the mean inverse participation ratio and mean fractal dimension, $\text{MIPR} = \sum_n (\text{IPR}_n)/L$ and $\text{MFD} = \sum_n (\text{FD}_n)/L$. Figure 3 shows their dependence on λ for different system sizes. In the extended regime, $\text{MIPR} \rightarrow 0$ and $\text{MFD} \rightarrow 1$ as L increases, while in the localized regime MIPR remains finite and $\text{MFD} \rightarrow 0$. In contrast, both quantities remain take intermediate values in the critical regime, consistent with multifractal scaling.

The localization transition can be determined analytically using Avila's global theory for quasiperiodic $SL(2, \mathbb{C})$ cocycles [89]. The transfer matrix defines an analytic cocycle $(\alpha, T_E(\theta))$ and the Lyapunov exponent admits the phase-averaged representation

$$\gamma(E) = \lim_{N \rightarrow \infty} \frac{1}{N} \int_0^{2\pi} \ln \|T_E[\theta + (N-1)\alpha] \cdots T_E(\theta)\| \frac{d\theta}{2\pi}. \quad (12)$$

Analytically continuing $\theta \rightarrow \theta + iy$ with $y \in \mathcal{R}$, we obtain the exact result [82]

$$\gamma(E) = \max \left\{ 0, \ln \frac{|\lambda|}{2|w|} \right\}. \quad (13)$$

Importantly, $\gamma(E)$ is independent of energy, implying the absence of mobility edges. For $|\lambda| > 2|w|$, $\gamma(E) > 0$ and all eigenstates are localized. For $|\lambda| < 2|w|$, $\gamma(E) = 0$, and the states are either extended or critical.

The distinction between extended and critical phases is controlled by the competition between v and λ . When $|\lambda| < |v|$, the spectrum is absolutely continuous and all states are extended. For $|v| < |\lambda| < 2|w|$, the spectrum becomes singular continuous [90], and all eigenstates are multifractal. Physically, the critical regime originates from incommensurate zeros in the effective hopping amplitudes when $|\lambda| > |v|$ [91, 92].

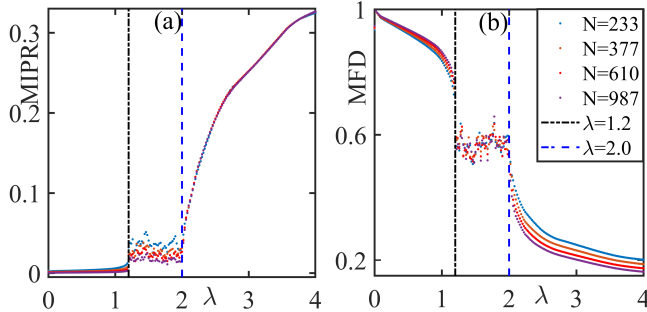


FIG. 3. (Color online) (a) Mean inverse participation ratio (MIPR) and (b) mean fractal dimension (MFD) as functions of the nonreciprocity strength λ for different system sizes. The black dot-dashed and blue dashed lines mark the analytical phase boundaries separating the extended-critical and critical-localized regimes, respectively. Parameters: $v = 1.2$ and $w = 1$.

The system therefore exhibits three different phases

$$\begin{cases} \text{extended phase:} & 0 < |\lambda| < |v|, \\ \text{critical phase:} & |v| < |\lambda| < 2|w|, \\ \text{localized phase:} & |\lambda| > 2|w|. \end{cases} \quad (14)$$

The resulting phase diagram is shown in Fig. 2(b). Comparing with the TAI diagram in Fig. 2(a), we uncover a finite parameter region where the topologically nontrivial phase overlaps with the multifractal critical regime. Along the representative cut $v = 1.2$ [black dashed line in Fig. 2(b)], the system evolves as follows: starting from a trivial extended phase at $\lambda = 0$, increasing λ first induces a TAI phase with extended bulk states; further increasing λ drives the bulk into a multifractal critical phase while the zero-energy edge modes persist; finally, for $|\lambda| > 2|w|$, the system becomes localized and topologically trivial. Notably, the extended-critical phase transition at $|\lambda| = |v|$ coincides exactly with the real-complex spectral transition, establishing a direct correspondence between spectral topology and wave-function criticality. Moreover, the critical window shrinks as $|v|$ increases and disappears entirely for $|v| > 2|w|$.

Experimental realization.—Topoelectrical circuits have emerged as a versatile platform for simulating topological band structures and non-Hermitian phenomena [13–15]. We propose a circuit implementation of the non-Hermitian quasicrystal, schematically shown in Fig. 4. In the circuit network, nodes represent lattice sites of the SSH chain. The capacitors C_1 and C_2 realize the intra- and intercell hopping amplitudes, respectively. Nonreciprocal intracell hopping is implemented using negative-impedance converters with current inversion (INICs), whose direction-dependent impedance Z_j generates the asymmetric hopping terms. By appropriately designing Z_j s and Z'_j , the circuit Laplacian \mathbf{J} defined through $\mathbf{I} = \mathbf{JV}$ (with \mathbf{I} and \mathbf{V} the nodal current and voltage vectors), reproduces the effective Hamiltonian in

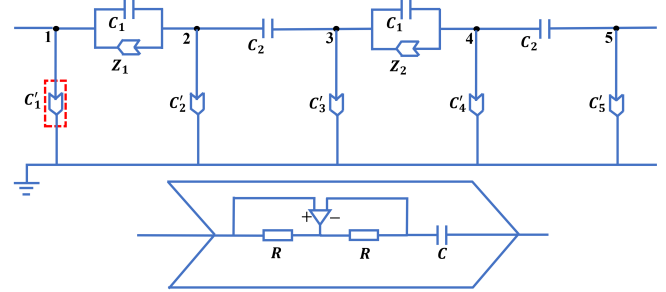


FIG. 4. (Color online) Schematic of the topoelectrical circuit realizing the non-Hermitian quasicrystal. The numbered black nodes represent lattice sites of the SSH chain. Capacitive couplings implement the Hermitian hopping terms, while the element highlighted in red denotes a negative-impedance converter with current inversion (INIC), which generates direction-dependent (nonreciprocal) intracell hopping. The effective impedances Z_j and Z'_j are controlled by the orientation of the INIC. The lower panel illustrates the internal structure of the INIC, whose impedance depends on the direction of the current flow.

Eq. (1) [82]. Topological and localization properties can be probed via impedance measurements. In particular, zero-energy edge modes manifest as pronounced peaks in the two-point impedance at the boundaries, while the admittance spectrum directly reveals the real-complex spectral transition and the localization regimes predicted in this work.

Summary—We have introduced and analytically characterized a non-Hermitian SSH quasicrystal with quasiperiodically modulated nonreciprocity. The interplay between non-Hermiticity and quasiperiodicity gives rise to two intertwined phenomena: a disorder-induced non-Hermitian TAI and a cascade of extended-critical-localized transitions. Most notably, we uncover a finite parameter regime where the TAI phase coexists with a multifractal critical bulk—an effect absent in previously studied disordered topological systems. We establish exact analytical phase boundaries and demonstrate that the extended-critical transition coincides precisely with the real-complex spectral transition, revealing a direct correspondence between spectral feature and wave-function criticality. The proposed topoelectrical circuit implementation offers an experimentally accessible route to probe these multifractal topological states. More broadly, quasiperiodic nonreciprocity provides a general mechanism for engineering hybrid quantum phases in which topology, non-Hermiticity, and criticality are intrinsically intertwined.

Acknowledgments.—This work is supported by the National Natural Science Foundation of China (Grant No. 12204326). R.L. is supported by the Quantum Science and Technology-National Science and Technology Major Project (Grant No. 2021ZD0302100) and the 'Gravitational Wave Detection' program (2023YFC2205800)

funded by the Ministry of Science and Technology of the People's Republic of China.

* zengqibo@cnu.edu.cn

- [1] M. Z. Hasan and C. L. Kane, Colloquium: Topological insulators, *Rev. Mod. Phys.* **82**, 3045 (2010).
- [2] X.-L. Qi and S.-C. Zhang, Topological insulators and superconductors, *Rev. Mod. Phys.* **83**, 1057 (2011).
- [3] N. P. Armitage, E. J. Mele, and A. Vishwanath, Weyl and Dirac semimetals in three-dimensional solids, *Rev. Mod. Phys.* **90**, 015001 (2018).
- [4] H. Cao and J. Wiersig, Dielectric microcavities: Model systems for wave chaos and non-Hermitian physics, *Rev. Mod. Phys.* **87**, 61 (2015).
- [5] V. V. Konotop, J. Yang, and D. A. Zezyulin, Nonlinear waves in PT-symmetric systems, *Rev. Mod. Phys.* **88**, 035002 (2016).
- [6] Y. Ashida, Z. Gong, and M. Ueda, Non-Hermitian physics, *Adv. Phys.* **69**, 249 (2020).
- [7] E. J. Bergholtz, J. C. Budich, and F. K. Kunst, Exceptional topology of non-Hermitian systems, *Rev. Mod. Phys.* **93**, 015005 (2021).
- [8] C. M. Bender and S. Boettcher, Real spectra in non-Hermitian Hamiltonians having PT symmetry, *Phys. Rev. Lett.* **80**, 5243 (1998).
- [9] C. M. Bender, Making sense of non-Hermitian Hamiltonians, *Rep. Prog. Phys.* **70**, 947 (2007).
- [10] V. Kozii and L. Fu, Non-Hermitian topological theory of finite-lifetime quasiparticles: prediction of bulk Fermi arc due to exceptional point, [arXiv:1708.05841](https://arxiv.org/abs/1708.05841).
- [11] Z. H. Musslimani, K. G. Makris, R. El-Ganainy, and D. N. Christodoulides, Optical solitons in PT periodic potentials, *Phys. Rev. Lett.* **100**, 030402 (2008).
- [12] L. Feng, R. El-Ganainy, and L. Ge, Non-Hermitian photonics based on parity-time symmetry, *Nat. Photonics* **11**, 752 (2017).
- [13] K. F. Luo, J. J. Feng, Y. X. Zhao, and R. Yu, Nodal manifolds bounded by exceptional points on non-Hermitian honeycomb lattices and electrical-circuit realization, [arXiv:1810.09231](https://arxiv.org/abs/1810.09231).
- [14] C. H. Lee, S. Imhof, C. Berger, F. Bayer, J. Brehm, L. W. Molenkamp, T. Kiessling, and R. Thomale, Topoelectrical circuits, *Commun. Phys.* **1**, 39 (2018).
- [15] H. Sahin, M. B. A. Jalil, C. H. Lee, Topoelectrical circuits-recent experimental advances and developments, [arXiv:2502.18563](https://arxiv.org/abs/2502.18563).
- [16] W. D. Heiss, The physics of exceptional points, *J. Phys. A: Math. Theor.* **45**, 444016 (2012).
- [17] H. Hu and E. Zhao, Knots and non-Hermitian Bloch bands, *Phys. Rev. Lett.* **126**, 010401 (2021).
- [18] K. Wang, A. Dutt, C. C. Wojcik, and S. Fan, Topological complex-energy braiding of non-Hermitian bands, *Nature* **598**, 59 (2021).
- [19] Z. Zhou, Z.-C. Xu, and L.-J. Lang, Non-Abelian geometry, topology, and dynamics of a nonreciprocal Su-Schrieffer-Heeger ladder, *Phys. Rev. B* **112**, 094305 (2025).
- [20] S. Yao and Z. Wang, Edge states and topological invariants of non-Hermitian systems, *Phys. Rev. Lett.* **121**, 086803 (2018).
- [21] S. Yao, F. Song, and Z. Wang, Non-Hermitian Chern bands, *Phys. Rev. Lett.* **121**, 136802 (2018).
- [22] N. Okuma, K. Kawabata, K. Shiozaki, and M. Sato, Topological origin of non-Hermitian skin effects, *Phys. Rev. Lett.* **124**, 086801 (2020).
- [23] K. Zhang, Z. Yang, and C. Fang, Correspondence between winding numbers and skin modes in non-Hermitian systems, *Phys. Rev. Lett.* **125**, 126402 (2020).
- [24] P. W. Anderson, Absence of diffusion in certain random lattices, *Phys. Rev.* **109**, 1492 (1958).
- [25] J. Li, R.-L. Chu, J. K. Jain, and S.-Q. Shen, Topological Anderson insulator, *Phys. Rev. Lett.* **102**, 136806 (2009).
- [26] C. W. Groth, M. Wimmer, A. R. Akhmerov, J. Tworzydło, and C. W. J. Beenakker, Theory of the topological Anderson insulator, *Phys. Rev. Lett.* **103**, 196805 (2009).
- [27] Y. Xing, L. Zhang, and J. Wang, Topological Anderson insulator phenomena, *Phys. Rev. B* **84**, 035110 (2011).
- [28] H. Jiang, L. Wang, Q.-F. Sun, and X. C. Xie, Numerical study of the topological Anderson insulator in HgTe/CdTe quantum wells, *Phys. Rev. B* **80**, 165316 (2009).
- [29] Y.-Y. Zhang, R.-L. Chu, F.-C. Zhang, and S.-Q. Shen, Localization and mobility gap in the topological Anderson insulator, *Phys. Rev. B* **85**, 035107 (2012).
- [30] J. Song, H. Liu, H. Jiang, Q.-F. Sun, and X. C. Xie, Dependence of topological Anderson insulator on the type of disorder, *Phys. Rev. B* **85**, 195125 (2012).
- [31] A. Atland, D. Bagrets, L. Fritz, A. Kamenev, and H. Schmiedt, Quantum criticality of quasi-one-dimensional topological Anderson insulators, *Phys. Rev. Lett.* **112**, 206602 (2014).
- [32] I. Mondragon-Shem and T. L. Hughes, Topological criticality in the chiral-symmetric AIII class at strong disorder, *Phys. Rev. Lett.* **113**, 046802 (2014).
- [33] Z.-Q. Zhang, B.-L. Wu, J. Song, and H. Jiang, Topological Anderson insulator in electric circuits, *Phys. Rev. B* **100**, 184202 (2019).
- [34] H.-C. Hsu and T.-W. Chen, Topological Anderson insulating phases in the long-range Su-Schrieffer-Heeger model, *Phys. Rev. B* **102**, 205425 (2020).
- [35] G.-G. Liu, et al. Topological Anderson insulator in disordered photonic crystals, *Phys. Rev. Lett.* **125**, 133603 (2020).
- [36] G.-Q. Zhang, L.-Z. Tang, L.-F. Zhang, D.-W. Zhang, and S.-L. Zhu, Connecting topological Anderson and Mott insulators in disordered interacting fermionic systems, *Phys. Rev. B* **104**, L161118 (2021).
- [37] Z. Lu, Z. Xu, and Y. Zhang, Exact mobility edges and topological Anderson insulating phase in a slowly varying quasiperiodic model, *Ann. Phys. (Berlin)* **534**, 2200203, (2022).
- [38] M. Ren, et al. Realization of gapped and ungapped photonic topological Anderson insulators, *Phys. Rev. Lett.* **132**, 066602 (2024).
- [39] X.-D. Chen, et al. Realization of time-reversal invariant photonic topological Anderson insulators, *Phys. Rev. Lett.* **133**, 133802 (2024).
- [40] R. Ji, Y. Zhang, S. Chen, and Z. Xu, Controllable emergence of multiple topological Anderson insulator phases in photonic Su-Schrieffer-Heeger lattices, [arXiv:2512.06851](https://arxiv.org/abs/2512.06851).
- [41] X. Wang, L. Wang, and S. Chen, Topological Anderson insulator and reentrant topological transitions in a mo-

saic trimer lattice, [arXiv:2601.13760](https://arxiv.org/abs/2601.13760).

[42] N. Hatano and D. R. Nelson, Localization transitions in non-Hermitian quantum mechanics, *Phys. Rev. Lett.* **77**, 570 (1996).

[43] N. M. Shnerb and D. R. Nelson, Winding numbers, complex currents, and non-Hermitian localization, *Phys. Rev. Lett.* **80**, 5172 (1998).

[44] Z. Gong, Y. Ashida, K. Kawabata, K. Takasan, S. Higashikawa, and M. Ueda, Topological phases of non-Hermitian systems, *Phys. Rev. X* **8**, 031079 (2018).

[45] H. Jiang, L.-J. Lang, C. Yang, S.-L. Zhu, and S. Chen, Interplay of non-Hermitian skin effects and Anderson localization in nonreciprocal quasiperiodic lattices, *Phys. Rev. B* **100**, 054301 (2019).

[46] Q.-B. Zeng and Y. Xu, Winding numbers and generalized mobility edges in non-Hermitian systems, *Phys. Rev. Research* **2**, 033052 (2020).

[47] Y. Liu, Y. Wang, X. J. Liu, Q. Zhou, and S. Chen, Exact mobility edges, PT-symmetry breaking, and skin effect in one-dimensional non-Hermitian quasicrystals, *Phys. Rev. B* **103**, 014203 (2021).

[48] D.-W. Zhang, L.-Z. Tang, L.-J. Lang, H. Yan, and S.-L. Zhang, Non-Hermitian topological Anderson insulators, *Sci. China-Phys. Mech. Astron.* **63**, 267062 (2020).

[49] H. Liu, Z. Su, Z.-Q. Zhang, and H. Jiang, Topological Anderson insulator in two-dimensional non-Hermitian systems, *Chinese Phys. B* **29**, 050502 (2020).

[50] L.-Z. Tang, L.-F. Zhang, G.-Q. Zhang, and D.-W. Zhang, Topological Anderson insulators in two-dimensional non-Hermitian disordered systems, *Phys. Rev. A* **101**, 063612 (2020).

[51] L.-Z. Tang, S.-N. Liu, G.-Q. Zhang, and D.-W. Zhang, Topological Anderson insulators with different bulk states in quasiperiodic chains, *Phys. Rev. A* **105**, 063327 (2022).

[52] Q. Lin, T. Li, L. Xiao, K. Wang, W. Yi, and P. Xue, Observation of non-Hermitian topological Anderson insulator in quantum dynamics, *Nat. Commun.* **13**, 3229 (2022).

[53] S. Aubry and G. André, *Ann. Isr. Phys. Soc.* **3**, 133 (1980).

[54] P. G. Harper, Single band motion of conduction electrons in a uniform magnetic field, *Proc. Phys. Soc. A* **68**, 874 (1955).

[55] S. Das Sarma, S. He, and X. C. Xie, Mobility edge in a model one-dimensional potential, *Phys. Rev. Lett.* **61**, 2144 (1988).

[56] F. M. Izrailev and A. A. Krokhin, Localization and the mobility edge in one-dimensional potentials with correlated disorder, *Phys. Rev. Lett.* **82**, 4062 (1999).

[57] S. Ganeshan, J. H. Pixley, and S. Das Sarma, Nearest neighbor tight binding models with an exact mobility edge in one dimension, *Phys. Rev. Lett.* **114**, 146601 (2015).

[58] X. Deng, S. Ray, S. Sinha, G. V. Shlyapnikov, and L. Santos, One-dimensional quasicrystals with power-law hopping, *Phys. Rev. Lett.* **123**, 025301 (2019).

[59] Y. Wang, X. Xia, L. Zhang, H. Yao, S. Chen, J. You, Q. Zhou, and X.-J. Liu, One-dimensional quasiperiodic mosaic lattice with exact mobility edges, *Phys. Rev. Lett.* **125**, 196604 (2020).

[60] T. T. Geisel and G. Petschel, New class of level statistics in quantum systems with unbounded diffusion, *Phys. Rev. Lett.* **66**, 1651 (1991).

[61] S. Y. Jitomirskaya, Metal-insulator transition for the almost mathieu operator, *Ann. Math.* **3**, 150 (1999).

[62] T. C. Halsey, M. H. Jensen, L. P. Kadanoff, I. Procaccia, and B. I. Shraiman, Fractal measures and their singularities: The characterization of strange sets, *Phys. Rev. A* **33**, 1141 (1986).

[63] A. D. Mirlin, Y. V. Fyodorov, A. Mildenberger, and F. Evers, Exact relations between multifractal exponents at the Anderson transition, *Phys. Rev. Lett.* **97**, 046803 (2006).

[64] Y. Wang, C. Cheng, X.-J. Liu, and D. Yu, Many-body critical phase: extended and nonthermal, *Phys. Rev. Lett.* **126**, 080602 (2021).

[65] Y. Wang, L. Zhang, S. Niu, D. Yu, and X.-J. Liu, Realization and detection of nonergodic critical phases in an optical Raman lattice, *Phys. Rev. Lett.* **125**, 073204 (2020).

[66] T. Xiao, D. Xie, Z. Dong, T. Chen, W. Yi, and B. Yan, Observation of topological phase with critical localization in a quasi-periodic lattice, *Sci. Bull.* **66**, 2175 (2021).

[67] H. Li, et al. Observation of critical phase transition in a generalized Aubry-André-Harper model with superconducting circuits, *npj Quantum Inf* **9**, 40 (2023).

[68] A. Pal and D. A. Huse, Many-body localization phase transition, *Phys. Rev. B* **82**, 174411 (2010).

[69] R. Nandkishore and D. A. Huse, Many-body localization and thermalization in quantum statistical mechanics, *Annu. Rev. Condens. Matter Phys.* **6**, 15 (2015).

[70] A. Purkayastha, S. Sanyal, A. Dhar, and M. Kulkarni, Anomalous transport in the Aubry-André-Harper model in isolated and open systems, *Phys. Rev. B* **97**, 174206 (2018).

[71] D. A. Abanin, E. Altman, I. Bloch, and M. Serbyn, Colloquium: Many-body localization, thermalization, and entanglement, *Rev. Mod. Phys.* **91**, 021001 (2019).

[72] L.-J. Lang, X. Cai, and S. Chen, Edge states and topological phases in one-dimensional optical superlattices, *Phys. Rev. Lett.* **108**, 220401 (2012).

[73] Y. E. Kraus, Y. Lahini, Z. Ringel, M. Verbin, and O. Zilberberg, Topological states and adiabatic pumping in quasicrystals, *Phys. Rev. Lett.* **109**, 106402 (2012).

[74] Y. E. Kraus and O. Zilberberg, Topological equivalence between the Fibonacci quasicrystal and the Harper model, *Phys. Rev. Lett.* **109**, 116404 (2012).

[75] S. Ganeshan, K. Sun, and S. Das Sarma, Topological zero-Energy modes in gapless commensurate Aubry-André-Harper models, *Phys. Rev. Lett.* **110**, 180403 (2013).

[76] X. Cai, L.-J. Lang, S. Chen, and Y. Wang, Topological superconductor to Anderson localization transition in one-dimensional incommensurate lattices, *Phys. Rev. Lett.* **110**, 176403 (2013).

[77] J. Wang, X.-J. Liu, G. Xianlong, and H. Hu, Phase diagram of a non-Abelian Aubry-André-Harper model with p-wave superfluidity, *Phys. Rev. B* **93**, 104504 (2016).

[78] Q.-B. Zeng, S. Chen, and R. Lü, Generalized Aubry-André-Harper model with p-wave superconducting pairing, *Phys. Rev. B* **94**, 125408 (2016).

[79] Q.-B. Zeng, Y.-B. Yang, and Y. Xu, Topological phases in non-Hermitian Aubry-André-Harper models, *Phys. Rev. B* **101**, 020201(R) (2020).

[80] Q.-B. Zeng and R. Lü, Topological phases and Anderson localization in off-diagonal mosaic lattices, *Phys. Rev. B* **104**, 064203 (2021).

[81] Q.-B. Zeng and R. Lü, Real spectra and phase transition of skin effect in nonreciprocal systems, *Phys. Rev. B* **105**, 245407 (2022).

[82] Supplementary material.

[83] A. Mostafazadeh, Pseudo-Hermiticity versus PT symmetry: The necessary condition for the reality of the spectrum of a non-Hermitian Hamiltonian, *J. Math. Phys.* **43**, 205 (2002).

[84] Q.-B. Zeng, Y.-B. Yang, and R. Lü, Topological phases in one-dimensional nonreciprocal superlattices, *Phys. Rev. B* **101**, 125418 (2020).

[85] H. Weyl, Ueber die gleichverteilung von zahlen mod. eins, *Math. Ann.* **77**, 313 (1916).

[86] G. H. Choe, Ergodicity and irrational rotations, *Proc. R. Ir. Acad., Sect. A* **93A**, 193 (1993).

[87] S. Longhi, Metal-insulator phase transition in a non-Hermitian Aubry-André-Harper model, *Phys. Rev. B* **100**, 125157 (2019).

[88] F. Song, S. Yao, and Z. Wang, Non-Hermitian topological invariants in real space, *Phys. Rev. Lett.* **123**, 246801 (2019).

[89] A. Avila, Global theory of one-frequency Schrödinger operators, *Acta. Math.* **1**, 215 (2015).

[90] A. Avila, S. Jitomirskaya, and C. A. Marx, Spectral theory of extended Harper's model and a question by Erdős and Szekeres, *Inventiones Mathematicae* **210**, 283 (2017).

[91] B. Simon and T. Spencer, Trace class perturbations and the absence of absolutely continuous spectra, *Commun. Math. Phys.*, **125**, 113 (1989).

[92] S. Jitomirskaya and C. A. Marx, Analytic quasi-periodic cocycles with singularities and the Lyapunov exponent of extended Harper's model, *Commun. Math. Phys.* **316**, 237 (2012).